Antiferromagnetism in Mn_5Si_3: the magnetic structure of the AF2 phase at 70 K

1995 J. Phys.: Condens. Matter 7 7619

(http://iopscience.iop.org/0953-8984/7/39/004)

J. Phys.: Condens. Matter 7 (1995) 7619–7628. Printed in the UK

Antiferromagnetism in Mn_5Si_3: the magnetic structure of the AF2 phase at 70 K

P J Brown† and J B Forsyth‡

† Institut Laue Langevin, BP 156, 38042 Grenoble Cédex, France

‡ Rutherford Appleton Laboratory, Chilton, Oxfordshire OX11 0QX, UK

Received 5 June 1995

Abstract. The antiferromagnetic structure of the AF2 phase of Mn_5Si_3, stable between the Néel point at 99 K and the transition to a second antiferromagnetic AF1 phase at 66 K, has been determined from unpolarized neutron integrated intensity measurements on single-crystal and powder samples. The paramagnetic phase adopts the hexagonal $D8_8$ structure, $Z = 2$, with Mn1 and Mn2 atoms in a fourfold and a sixfold site respectively. With the onset of long-range magnetic order the symmetry is reduced to orthorhombic. The orthorhombic cell dimensions at 70 K are $a = 6.898\,56(1)$, $b = 11.891\,20(2)$ and $c = 4.793\,30(1)$ Å and these are related to those of the hexagonal cell, a_h etc, by $a \approx a_h$, $b \approx \sqrt{3}a_h$ and $c \approx c_h$. The orthorhombic cell is C-face centred, space group *Ccmm*, with $Z = 4$. Magnetic reflections indexed on this cell have $h + k$ odd corresponding to a (010) magnetic propagation vector. Zero-field neutron polarimetry on a single crystal shows that there are no components of moment parallel to the c axis. A magnetic structure in which the Mn1 and one-third of the Mn2 atoms have no ordered moment and the remaining Mn2 atoms a moment of $1.48(1)\mu_B$ directed parallel and antiparallel to *b* gives a good fit to both the powder and single-crystal intensities. This structure differs significantly from previous models, but it is coherent with current ideas about the stability of Mn moments in compounds with B-subgroup elements. Its relation to the recently revised structure of the low-temperature AF1 phase is discussed.

1. Introduction

The factors which govern the occurrence of long-range magnetic order amongst manganese atoms in the element and its intermetallic compounds have been the subject of discussion for more than a hundred years, stimulated in the first instance by Heusler's discovery of ferromagnetism in the alloy Cu_2MnAl [1]. In the last decade the importance of Mn–Mn interatomic distances and frustration in determining the occurrence, magnitude and stability of the ordered moments has been increasingly recognized. Much of this work has targeted compunds of manganese with rare earth elements and less attention has been paid to its compounds with the B-subgroup elements.

It was in 1968 that we first reported antiferromagnetism in the compound Mn_5Si_3 which at ambient temperatures has the $D8_8$ structure illustrated in figure 1. The unit cell is hexagonal with space group $P6_3/mcm$. The unit cell parameters at 300 K are $a = 6.910$, $c = 4.814$ Å with $Z = 2$ [2]. The atomic positions [2, 3] are

Mn1 in 4(d) sites at $\pm(\frac{1}{3}, \frac{2}{3}, 0; \frac{2}{3}, \frac{1}{3}, \frac{1}{2})$

Mn2 in 6(g) sites at $\pm(x, 0, \frac{1}{4}; 0, x, \frac{1}{4}; -x, -x, \frac{1}{4})$ with $x = 0.2360(1)$

Si in 6(g) sites at $\pm(x, 0, \frac{1}{4}; 0, x, \frac{1}{4}; -x, -x, \frac{1}{4})$ with $x = 0.5991(2)$.

0953-8984/95/397619+10$19.50

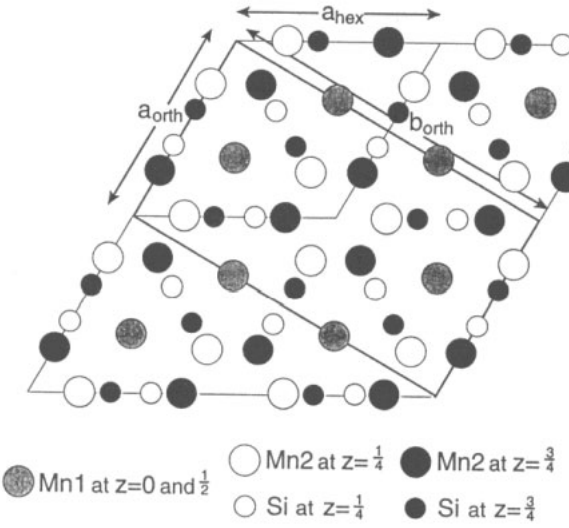

Figure 1. [001] projection of the structure of Mn_5Si_3. Four hexagonal unit cells are shown. The orthohexagonal unit cell which is the basis for the orthorhombic cell used to describe the magnetic structure is outlined with bold lines.

At 4.2 K, the magnetic propagation vector referred to the hexagonal cell is $\frac{1}{2}$ 0 0 and the structure was described in terms of an orthohexagonal cell with $a \approx a_h$, $b \approx \sqrt{3}a_h$ and $c \approx c_h$, where a_h and c_h refer to the hexagonal cell dimensions. Rather surprisingly, the single-crystal neutron study provided incontrovertible evidence that one-third of the Mn2 atoms carry no ordered moment in the magnetic structure at 4.2 K, whereas the other two-thirds do [4]. The magnitudes found for the ordered moments were 0.60(6) and 1.14(8)μ_B for the Mn1 and Mn2 atoms, respectively.

Later investigations [5, 6] showed that the temperature of 66 K, believed by [4] to be the Néel point of Mn_5Si_3, only marks the transition from the low-temperature AF1 structure to a second antiferromagnetically ordered AF2 phase and that the true Néel temperature is at about 100 K. It was further found from x-ray diffraction measurements that the transition at 100 K is accompanied by an orthorhombic distortion of the hexagonal unit cell.

The first magnetic model for the AF2 phase was proposed by Povzner *et al* [7] in 1978 on the basis of neutron powder data collected at 80 K. An incident wavelength of 1.07 Å was used but the diffractometer was of so low a resolution that only two pairs of overlapped lines were available for interpretation. In their model, only the Mn1 atoms carry ordered moments and these are parallel and antiparallel to the long orthorhombic **b** axis with ferromagnetic coupling between pairs of atoms **c**/2 apart. The (010) magnetic propagation vector implies that moments on atoms related by the C-face centring of the orthorhombic cell are antiparallel. This structure is illustrated in figure 2(*a*). The magnitude of the Mn1 moment was estimated to be 1.8μ_B.

Further x-ray measurements of the cell dimensions of a single-crystal sample showed that the AF2–AF1 transition at 66 K is also associated with a discontinuity in the *c* dimension and a change in *b* from being somewhat less than $\sqrt{3}a_h$ above 66 K to being somewhat greater than $\sqrt{3}a_h$ below [8]. These observations are reproduced in figure 3. In 1990, alternative models for both the AF1 and AF2 phases were put forward by Menshikov *et al* [9] based mainly on new neutron powder diffraction data obtained at 1.81 Å with a somewhat improved instrumental resolution. Even so, the two pairs of lowest-angle magnetic lines

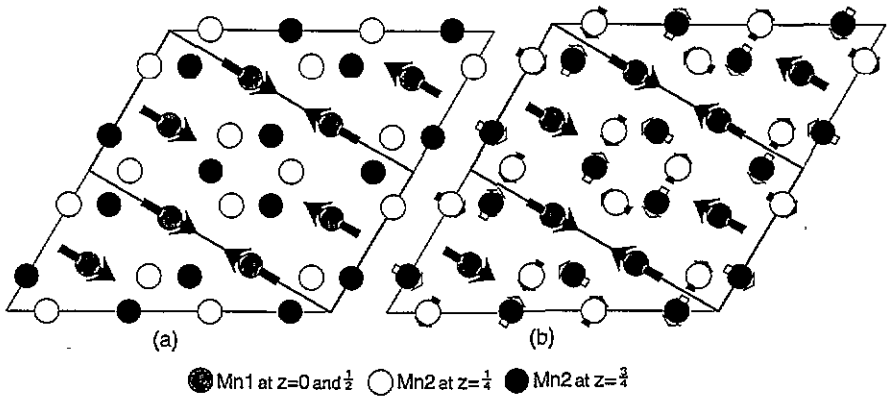

Figure 2. The general motif for the high-temperature structure AF2 of Mn_5Si_3 (*a*) proposed by [7] and (*b*) proposed by [9]. The moments on the Mn1 atoms at z = 0 are parallel to those on the atoms at $z = \frac{1}{2}$.

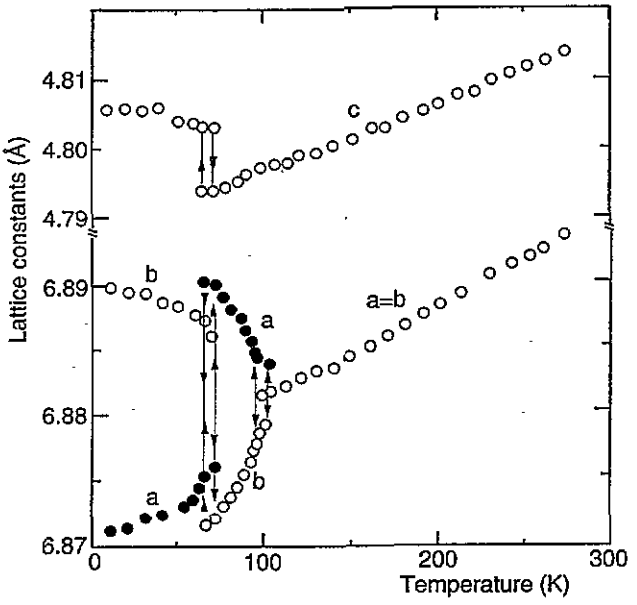

Figure 3. The temperature variation of the cell dimensions of Mn_5Si_3 as determined by x-ray diffraction and reported by [8].

were still not resolved, though the data did extend to $\sin\theta/\lambda = 0.24$ Å^{-1}. These authors again confined all moments in the AF2 phase to the *a*–*b* plane of the orthorhombic cell, but in their model all Mn1 and Mn2 atoms carry ordered moments. The coupling scheme and directions for the Mn1 moments adopted by [7] are retained but the moment value is reduced to $1.6(1)\mu_B$. One-third of the Mn2 atoms also have moments parallel and antiparallel to *b* but the remaining two-thirds are parallel and antiparallel to *a*. All Mn2 atoms carry an equal moment of $0.8(1)\mu_B$. This model is shown in figure 2(*b*) and the components of moment on the various Mn sublattices in both the earlier models are given in table 1. In the model of the same authors for the AF1 phase all Mn atoms again have ordered moments

Table 1. Definition of the labels for the different Mn sublattices in Mn_5Si_3 and the different couplings between the moments on them which have been proposed for the AF2 structure. The atomic positions and the x, y components of moment M_x, M_y in μ_B are given on the orthorhombic axes defined in the text. All z components of moment are zero. Only one half of the atoms in the unit cell are given, the other half are displaced by $(\frac{1}{2}, \frac{1}{2}, 0)$ and have antiparallel moments.

		Povsner *et al* [7]		Menshikov *et al* [9]		New model	
Atom	Position	M_x	M_y	M_x	M_y	M_x	M_y
	$(0, \frac{1}{3}, 0)$	0	1.8	0	2.45	0	0
Mn1	$(0, \frac{1}{3}, \frac{1}{2})$	0	1.8	0	2.45	0	0
	$(0, \frac{1}{6}, 0)$	0	1.8	0	2.45	0	0
	$(0, \frac{1}{6}, \frac{1}{2})$	0	1.8	0	2.45	0	0
Mn21	$(x_1, 0, \frac{1}{4})$	0	0	0	1.1	0	0
	$(\bar{x}_1, 0, \frac{1}{4})$	0	0	0	1.1	0	0
	$(x_2, y_2, \frac{3}{4})$	0	0	−1.1	0	0	1.48
	$(\bar{x}_2, \bar{y}_2, \frac{1}{4})$	0	0	−1.1	0	0	1.48
Mn22	$(x_2, \bar{y}_2, \frac{3}{4})$	0	0	1.1	0	0	−1.48
	$(\bar{x}_2, y_2, \frac{1}{4})$	0	0	1.1	0	0	−1.48
	$x_1 = 0.2394$, $x_2 \approx x_1/2$ and $y_2 \approx x_2$						

with the magnitude of the Mn1 moment remaining larger than that of Mn2 (2.45:1.1μ_B, respectively).

The development of zero-field polarimetry [10–12] has allowed us to supplement the early single-crystal integrated intensity measurements on the AF1 phase [4] and has led to a recent revision of its structure [13]. The polarimetry data proved critical in distinguishing between models which gave similar agreement factors on the basis of integrated intensity measurements alone. We now report a new model for the AF2 structure at 70 K based on unpolarized neutron integrated intensity measurements on single-crystal and powder samples and on further single-crystal polarimetry observations.

2. Neutron powder diffractometry

Time of flight powder diffraction patterns were taken using backward angle detectors on both the high-resolution instrument HRPD on ISIS, which views the methane moderator at 90 K, and the IRIS spectrometer on the same source which receives neutrons from the liquid hydrogen moderator at 20 K. The former instrument, with an incident flight path of 95 m and a 1 m specimen to detector distance, has an excellent resolution; $\Delta/d < 10^{-3}$, and can provide data which extend down to d-spacings of 0.3 Å. It has however a rather low incident flux of neutrons with wavelengths > 6 Å. The diffraction detector on IRIS has complementary characteristics with a 35 m incident flight path, a 0.85 m specimen to detector distance, a resolution $\Delta/d = 2.5 \times 10^{-3}$ and a high flux of cold neutrons with which to measure d-spacings in the range 2.5–12 Å. In these conditions, the lower limit of measurable d-spacing is set by the Bragg cut-off of the aluminium windows in the specimen tank and the tails of cryostat being used.

HRPD data in the tof range 30–230 ms were collected at 70 and 5 K, temperatures which are within the stability ranges of the AF2 and AF1 phases respectively. The two subsets into which the nuclear reflections are split by the distortion of the orthohexagonal

cell were almost completely resolved at the longer times of flight and the crossover of the b cell dimension from being somewhat less than $\sqrt{3}a_h$ at 70 K to being somewhat greater than $\sqrt{3}a_h$ at 5 K was confirmed. Data in the tof range 36–170 ms, normalized and corrected using a vanadium standard, were used for Rietveld refinement of the nuclear structure of the AF2 phase within the space group *Ccmm*. This gave the parameters reported in table 2. It should be noted that with this symmetry the Mn1 atoms occupy a single eightfold site, whereas the Mn2 atoms occupy one fourfold and one eightfold site, breaking the equivalence which they have in the hexagonal paramagnetic phase. The c and the mean of the a and $b/\sqrt{3}$ dimensions (6.8820 Å) are in reasonable agreement with those reported by [8] and shown in figure 3, but the fractional distortion introduced by the phase transition to orthorhombic, $[a_h - b_h/\sqrt{3}]/a_h$, was found to be 4.81×10^{-3} at 70 K compared to the value of 2.56×10^{-3} reported in the x-ray study.

Table 2. Parameters of the crystal structure of Mn_5Si_3 at 70 K.

$a = 6.898\,56(1)$, $b = 11.891\,20(2)$, $c = 4.793\,30(1)$ Å. Space group *Ccmm*, $Z = 4$					
			Atomic positions: $(000; \frac{1}{2}\frac{1}{2}0)\pm$		
Mn1	8(e)	2	$x, 0, 0$;	$x, 0, \frac{1}{2}$	with $x = 0.3328(2)$
Mn21	4(c)	*mm*	$x, 0, \frac{1}{4}$		with $x = 0.2392(4)$
Mn22	8(g)	*m*	$x, y, \frac{1}{4}$;	$x, -y, \frac{1}{4}$	with $x = 0.8826(3)$, $y = 0.8820(2)$
Si1	4(c)	*mm*	$x, 0, \frac{1}{4}$		with $x = 0.5991(3)$
Si2	6(g)	*mm*	$x, y, \frac{1}{4}$;	$x, -y, \frac{1}{4}$	with $x = 0.7002(2)$, $y = 0.7000(1)$

Although the HRPD data contained some weak lines of magnetic origin, the magnetic scattering was not modelled in the initial nuclear structure refinements. The magnetic scattering makes a much more significant contribution to the IRIS powder patterns and these were used in the first instance to refine the magnetic structure parameters. Working at 25 Hz, the phasing choppers on IRIS can be set to allow different wavelength windows of width 3 Å onto the sample which in turn results in diffraction patterns each covering a range of 1.5 Å in d-spacing. Five successive overlapping ranges were collected from a flat plate powder sample of dimensions $40 \times 40 \times 3$ mm^3 contained in an aluminium can and held at 70 K in an ILL 'Orange' liquid helium cryostat: the total pattern extended from 2.5 to 12 Å in d. The instrumental resolution is still sufficient to show the orthorhombic splitting of the nuclear reflections.

3. Zero-field single-crystal neutron polarimetry

The polarization of the diffracted beam for a limited number of magnetic $\{hk0\}$ reflections was measured from a 1.03 g single crystal of Mn_5Si_3 kindly supplied by Dr A Z Menshikov of the Institute for Metal Physics, Ekaterinburg. The sample was held at 70 K in the CRYOPAD polarimeter [10] which was mounted on the IN20 polarized beam neutron spectrometer at the Institut Laue Langevin, Grenoble. The data were collected immediately after the measurements which were made at 4.2 K and which contributed critically to a revision of the AF1 magnetic structure [13]. In contrast to these latter observations, at 70 K none of the reflections showed the depolarization of the diffracted beam that had been observed at 4.2 K. This depolarization was due to the presence. in the AF1 structure, of domains arising from the absence of the mirror plane perpendicular to [001] and to the presence of an [001] component of magnetization. The absence of depolarization at 70 K

strongly suggests that the full orthorhombic symmetry is conserved in the AF2 structure and shows conclusively that the antiferromagnetic moments in the AF2 phase are confined to the (001) plane, as had indeed been assumed in the earlier models of Povzner *et al* [7] and Menshikov *et al* [9].

4. Unpolarized neutron single-crystal integrated intensities

Integrated intensity measurements were made on a small single crystal (≈ 3 mm^3) of Mn_5Si_3 cut from a corner of the larger crystal used for the polarimetry measurements. It was mounted in a standard ILL 'Orange' cryostat on the D15 diffractometer at ILL with a $[\bar{1}10]$ axis approximately parallel to the ω axis of the diffractometer. D15 was used in normal beam geometry with an incident neutron wavelength of 1.176 Å. Data were collected at 75 K for nuclear reflections $hk\ell$ with $-1 \leqslant h-k \leqslant 3$ and $\sin\theta/\lambda < 0.5$ Å^{-1}. Magnetic reflections occur at reciprocal lattice positions $hk\ell$ with either h or k or both half integer: their integrated intensities were measured in the same range of $h+k$ as above out to $\sin\theta/\lambda = 0.35$ Å^{-1}. The data were separated into three groups corresponding to the three orthohexagonal domains, re-indexed on the orthohexagonal cell and the intensities of equivalent reflections within each group averaged. Finally equivalent reflections from the different domains were compared and the relative domain populations derived. It was found that one of the three domains was about twice as populous as the other two. The domain populations were used to combine the data from the three domains to give a single set of magnetic structure factors which are listed in table 3; they have been put onto an absolute scale using the intensities of the nuclear reflections. It should be noted that no significant magnetic intensity was found in the $\{h0\ell\}$ reflections as was also the case in the single-crystal unpolarized neutron study of the AF1 phase [4]. Since the Mn21 atoms are not overlapping in the [010] projection, this observation leads directly to the conclusion that these atoms carry no ordered magnetic moment.

5. The AF2 antiferromagnetic structure of Mn_5Si_3

A striking feature of the both the IRIS powder diffraction pattern and the single-crystal measurements is the absence of the 010 magnetic reflection, which is strong in the AF1 phase. The most obvious way to incorporate this information into a model for the antiferromagnetic structure of the AF2 phase is to assume that it is collinear with the moments parallel and antiparallel to [010]. Assuming that the coupling scheme between the Mn moments is the same as that found in the AF1 phase, it remains to refine the magnitudes of their moments to obtain a fit to the IRIS powder pattern and to the single-crystal data. The excellent fit to the IRIS data illustrated in figure 4 corresponds to a model in which the Mn22 moment is $1.48(1)\mu_B$, but in which there is no ordered moment on either the Mn1 or the Mn21 sites. Refinement of this model using the single-crystal data gave a value of 1.47(2) for the Mn22 moment in close agreement with the powder refinement.

The same magnetic model was then introduced into the refinement of the HRPD powder profile over a restricted tof range from 70 to 170 ms which covered the stronger magnetic intensities. The fit was again good as shown in figure 5 with a Mn22 moment of $1.46(4)\mu_B$.

The magnetic symmetry of the proposed AF2 structure is orthorhombic as was predicted from the lack of depolarization due to domains in the polarimetric measurements. The magnetic group is $C'cm'm'$. In contrast the AF2 structure given by [7] has magnetic

Table 3. Comparison between the magnetic structure amplitudes obtained from single-crystal measurements at 75 K and those calculated for the models proposed by Povzner *et al* [7], Menshikov *et al* [9] and for the new structure proposed in this paper. The magnetic structure factors in units of 10^{-13} cm are tabulated up to $\sin\theta/\lambda = 0.3$ Å^{-1}.

$h\ k\ \ell$	$\sin\theta/\lambda$	Observed	Povsner *et al*	Menshikov *et al*	Present model
0 1 0	0.040	0.0(2)	0.00	0.00	0.41
1 0 0	0.070	0.15(4)	0.00	0.07	0.00
1 2 0	0.106	1.21(4)	1.94	1.88	1.19
0 1 1	0.107	1.82(3)	0.00	1.02	1.73
0 3 0	0.121	0.2(1)	0.00	0.00	0.29
1 0 1	0.121	0.1(1)	0.00	0.73	0.27
2 1 0	0.145	1.60(4)	2.56	2.46	1.60
1 2 1	0.145	1.7(1)	0.00	0.86	1.53
0 3 1	0.156	1.38(3)	0.00	1.05	1.21
1 4 0	0.175	0.35(4)	0.96	0.86	0.38
2 1 1	0.175	0.23(2)	0.00	0.10	0.25
2 3 0	0.184	1.5(1)	0.00	1.06	1.31
0 5 0	0.201	0.3(1)	0.00	0.00	0.31
1 4 1	0.201	0.3(1)	0.00	0.29	0.21
0 1 2	0.202	0.1(2)	2.13	1.98	0.27
3 0 0	0.209	0.33(5)	0.00	0.14	0.00
2 3 1	0.209	0.2(1)	0.00	0.06	0.13
1 0 2	0.210	0.32(4)	0.00	0.05	0.25
3 2 0	0.224	1.39(4)	1.85	1.70	1.37
0 5 1	0.224	0.49(4)	0.00	0.54	0.44
1 2 2	0.225	1.13(4)	1.84	1.77	1.16
3 0 1	0.231	0.1(1)	0.00	0.48	0.11
0 3 2	0.232	0.2(1)	0.00	0.42	0.20
2 5 0	0.244	0.53(3)	1.03	0.93	0.49
3 2 1	0.245	0.95(2)	0.00	0.35	0.96
2 1 2	0.245	1.1(1)	1.77	1.74	1.11
1 6 0	0.251	0.38(4)	0.00	0.57	0.24
3 4 0	0.264	0.1(2)	1.31	1.18	0.07
2 5 1	0.264	0.0(2)	0.00	0.08	0.24
1 4 2	0.264	0.33(4)	1.30	1.17	0.27
1 6 1	0.270	0.51(3)	0.00	0.68	0.50
2 3 2	0.270	1.1(1)	0.00	0.75	1.06
4 1 0	0.281	0.3(1)	1.49	1.38	0.19
3 4 1	0.281	0.2(1)	0.00	0.27	0.24
0 5 2	0.282	0.1(2)	1.05	0.98	0.22
3 0 2	0.288	0.1(2)	0.00	0.10	0.10
4 1 1	0.298	0.76(1)	0.00	0.17	0.85
0 7 1	0.298	0.5(1)	0.00	0.63	0.38
3 2 2	0.299	0.93(2)	1.33	1.26	0.98
0 1 3	0.300	0.78(3)	0.00	0.47	0.86

symmetry $C'c'm'm'$ whereas in that of [8] the mirror plane perpendicular to b is not present and the magnetic group is $C'c'2m'$. This latter structure does have two distinct orientation domains related by the missing mirror plane. In the magnetic group $C'cm'm'$ the symmetry does not constrain the magnetic moments to lie parallel to the orthorhombic b axis but allows them freedom to turn in the a–b plane so that each group of six Mn2 atoms has a resultant moment, antiferromagnetism being maintained by the reversal of this moment between the corners and face centres of the cell. If such canting were to exist and were large it would lead to significant scattering in the $h0\ell$ reflections. Such scattering from a small degree of canting might however be below the sensitivity of observation. To determine a

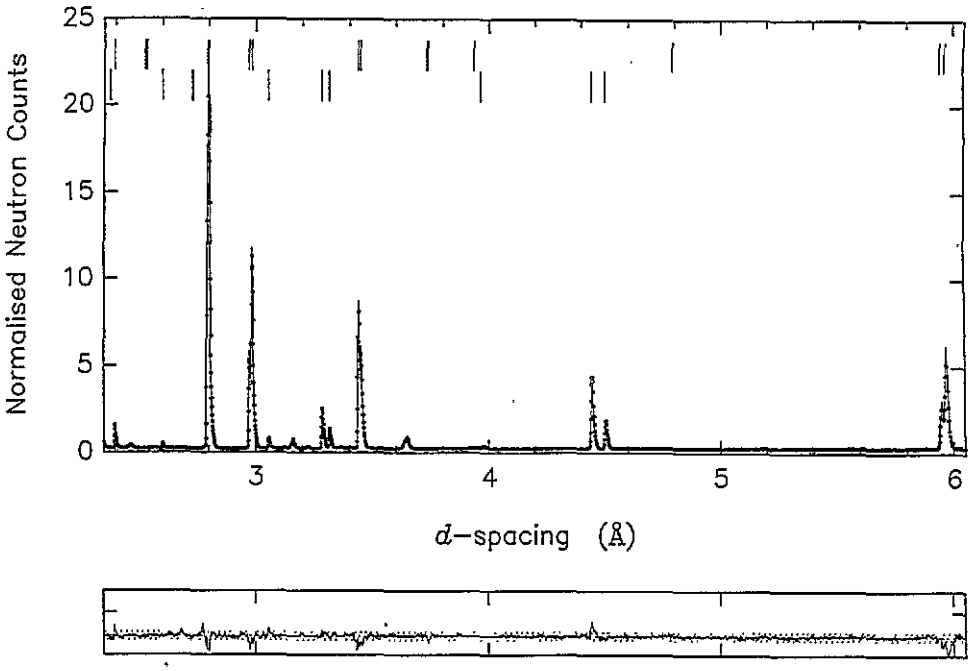

Figure 4. Rietveld profile fit to the IRIS data obtained at 70 K using the magnetic model described in the text and the atomic positional parameters of table 1. The upper set of markers refers to nuclear, the lower to magnetic reflections.

limit for such canting the single-crystal data were used in the refinement of a model which allowed a small moment parallel to a on the Mn21 sites and rotation of the Mn22 moments in the a–b plane. Although the results of this refinement suggested a rotation of some 10° of the Mn22 moments towards a, it did not improve the goodness of fit. It was therefore concluded that the best model for the structure was the one in which all moments are parallel to b and there is no moment on the Mn21 atoms. The magnetic structure factors for this model with $\mu = 1.48\mu_B$ for reflections with $\sin\theta/\lambda \leqslant 0.3$ Å^{-1} are given in table 3 where they can be compared with the observed structure factors and with those calculated from the models of [7] and [8]. The components of moment on the different Mn sublattices are listed in the last two columns of table 1

6. Discussion

The new model for the AF2 magnetic structure is illustrated in figure 6. In comparison to the earlier models illustrated in figure 2, two major differences emerge: firstly, the absence of ordered moment on the Mn1 sites which, in the model proposed by [7], were the only sites to carry such a moment and which still retained the larger ordered moment in the model proposed by [9]; secondly, and in common with the AF1 structure, the absence of moment on one-third of the Mn2 sites of the parent hexagonal paramagnetic phase. The failure of previous attempts to arrive at a correct structure for the AF2 phase is to a large extent due to the use of only relatively poorly resolved neutron powder data. The four largest d-spacing magnetic lines occur in two pairs, $120 + 011$ at $\sin\theta/\lambda = 0.1110$ and 0.1122 Å^{-1} respectively and $210 + 121$ at $\sin\theta/\lambda = 0.1511$ and 0.1522 Å^{-1}. These pairs

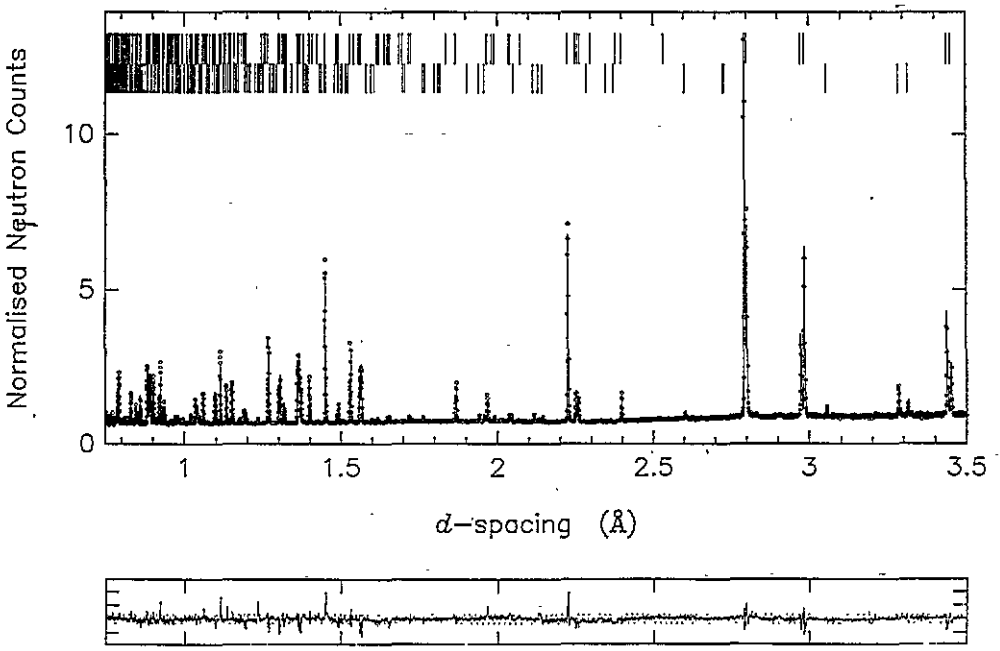

Figure 5. Rietveld profile fit to the HRPD data obtained at 70 K using the magnetic model described in the text and the atomic postional parameters of table 1. The upper set of markers refers to nuclear, the lower to magnetic reflections.

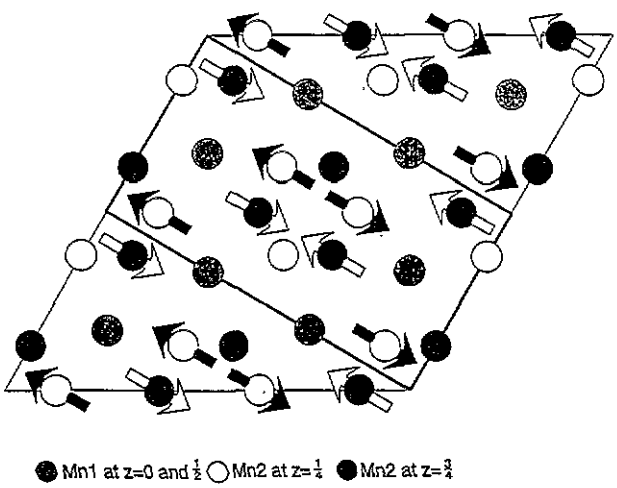

Figure 6. The [001] projection of the revised magnetic structure of the AF2 phase of Mn_5Si_3. The magnitude of the Mn22 moments is 1.48(1)μ_B at 70 K.

are completely unresolved in both earlier datasets but are completely resolved in the IRIS pattern. The AF1 structure proposed by Menshikov *et al* [9] predicts the two summed intensities correctly, but the division of intensity between their contributing reflections is seriously in error.

The suppression of an ordered moment on the Mn1 sites is probably associated with

the presence of two Mn1 neighbours at $\pm c/2$, an extremely short distance of 2.3967 Å. This separation is probably just below the limit required for stability of a Mn moment. The abrupt increase in the c cell dimension which accompanies the AF2–AF1 transition at 66 K is shown in figure 3 [8]. This change has the direct effect of relieving the chemical pressure exerted by the Mn1 atoms on each other as an ordered moment is established. In the AF1 phase at 4.2 K the Mn1 moments are $1.20(5)\mu_B$, with a Mn1–Mn1 $c/2$ separation of 2.4021 Å; the two-thirds of the Mn2 atoms which carry ordered moment are divided into two equal sets with moments of 1.85(9) and $2.30(9)\mu_B$ [13]. The inequality of ordered Mn moments in the $D8_8$ ferromagnet Mn_5Ge_3 and related phases has been discussed in [14], the authors of which correlate decreasing Mn moment with increasing number and proximity of Mn neighbours. In Mn_5Ge_3 itself the Mn1–Mn1 separation parallel to c is 2.522 Å and the Mn1 moment is $1.96(3)\mu_B$, but its magnitude remains notably smaller than the $3.23\mu_B$ exhibited by the Mn2 atoms.

An analysis has been made of the differences in bond lengths in the three phases from the cell dimensions and structural parameters obtained from refinement of high-resolution powder diffraction data. The orthorhombic distortion which accompanies the formation of the AF2 structure results in shortening the distances between antiferromagnetically coupled near-neighbour Mn2 atoms and most particularly that between atoms at the same height in the unit cell (−7%). The Mn1–Mn2 distances increase slightly so that there is no significant change in the unit cell volume. On transition to the AF1 phase, the Mn2–Mn2 bond distances expand and the hexagonal symmetry of the puckered ring of Mn2 atoms is largely restored. At the same time the Mn1–Mn2 distances contract. The distortion $b_{orth} < \sqrt{3}a_{orth}$ seems to be characteristic of the antiferromagnetic Mn2–Mn2 coupling scheme which leads to contraction of the bond distances between antiferromagnetically coupled near neighbours (the Mn22–Mn22 pairs at the same height in the cell). On lowering the temperature the crossover to $b_{orth} > \sqrt{3}a_{orth}$ is driven by the stabilization of Mn1 moments. The newly established magnetic coupling between the Mn1 and Mn2 systems results in shortened distances between Mn1–Mn2 near-neighbour pairs. The existence of both Mn1 and Mn2 ordered moments gives a more uniform distribution of moment in the unit cell. Finally due to the Mn2 spin reorientation there is no longer strict antiparallel coupling between near-neighbour Mn2 atoms which allows their separation to increase.

References

[1] Heusler F 1903 *Verh. Deutsch. Phys. Ges.* **5** 219
[2] Aronsson B 1960 *Acta. Chem. Scand.* **14** 1414
[3] Lander G H and Brown P J 1967 *Phil. Mag.* **16** 521
[4] Lander G H, Brown P J and Forsyth J B 1967 *Proc. Phys. Soc.* **91** 33
[5] Gel'd P V, Mikhel'son A V, Kalishevich G I, Krentis R P, Putintsev Yu V and Sudakova N P 1972 *Fiz. Tverd. Tela* **14** 930
[6] Gel'd P V, Kuznetsov S I, Krentis R P, Mikhel'son A V, Sudakova N P and Sheinker M E 1975 *Izv. Vyssh. Uchebn. Zaved. Fiz.* **11** 147
[7] Povzner A A, Sheinker M E, Krentsis R P and Gel'd P V 1978 *Izv. Vuzov, Fiz.* **5** 126 (Engl. Transl. *Sov. Phys. J.* **21** 654)
[8] Istomina Z A, Andreeva L P, Zadvorkin S M and Andreev A V 1983 *Fizicheskie svoistva metallov i splavov, Izd. Ural Polytechnic Institute, Sverdlovsk* p 13
[9] Menshikov A Z, Vokhmyanin A P and Dorofeev Yu A 1990 *Phys. Status Solidi* b **158** 319
[10] Tasset F 1989 *Physica* B **156–157** 627
[11] Brown P J, Chattopadhyay T, Forsyth J B, Nunez V and Tasset F 1991 *J. Phys.: Condens. Matter* **3** 4281
[12] Nunez V, Brown P J, Forsyth J B and Tasset F 1991 *Physica* B **174** 60
[13] Brown P J, Forsyth J B, Nunez V and Tasset F 1992 *J. Phys.: Condens. Matter* **4** 10 025